Ardeola 48(2), 2001, 161-173

ON THE ROLE OF THE ALULA IN THE STEADY FLIGHT OF BIRDS

J. C. ÁLVAREZ*[1], J. MESEGUER*, E. MESEGUER* & A. PÉREZ**

SUMMARY.—*On the role of the alula on the steady flight of birds*. The alula is a high lift device located at the leading edge of the birds wings that allows these animals to fly at larger angles of attack and lower speeds without wing stalling. The influence of the alula in the wing aerodynamics is similar, to some extent, to that of leading edge slats in aircraft wings, which are only operative during take-off and landing operations. In this paper, representative parameters of the wing geometry including alula position and size of forty species of birds, are reported. The analysis of the reported data reveals that both alula size and position depend on the aerodynamic characteristics (wing load and aspect ratio) of the wing. In addition, aiming to clarify if the alula is deflected voluntarily by birds or if the deflection is caused by pressure forces, basic experimental results on the influence of the wing aerodynamics on the mechanism of alula deflection at low velocities are presented. Experimental results seem to indicate that the alula is deflected by pressure forces and not voluntarily.

Key words: Alula, high lift devices, steady flight, wing load.

RESUMEN.—*El papel del álula en el vuelo estacionario de las aves*. El álula es un dispositivo hipersustentador situado en el borde de ataque de las alas de los pájaros que permite que estos animales vuelen a altos ángulos de ataque y bajas velocidades sin que se produzca la entrada en pérdida del ala (el ala deja de sustentar si el ángulo de ataque es muy grande). La influencia del álula en la aerodinámica de las alas es, hasta cierto punto, semejante a las aletas de borde de ataque que equipan las alas de las aeronaves, dispositivos que solo son operativos durante las operaciones de despegue y aterrizaje. En esta publicación se presenta información sobre los parámetros representativos de la geometría de las alas, incluidos el tamaño y la posición de las álulas de cuarenta especies de aves. El análisis de esta información revela que tanto la posición como el tamaño del álula dependen de las características del ala (carga alar y alargamiento). Además, con el fin de aclarar si el álula es deflectada voluntariamente por las aves o si la deflexión se produce por las fuerzas de presión, han sido llevados a cabo unos sencillos experimentos sobre la influencia de la aerodinámica del ala en el mecanismo de deflexión del álula a bajas velocidades. Los resultados experimentales parecen indicar que el álula es deflectada por las fuerzas de presión y no voluntariamente.

Palabras clave: Alula, carga alar, dispositivos hipersustentadores, vuelo estacionario.

INTRODUCTION

To analyse the flight of birds from an engineering point of view, in an extreme simplification of the problem, it can be said that birds can fly either by gliding or by flapping. In the former case-gliding, the flight path must be descendent (provided that the atmosphere is at rest). In this way, the component of the animal weight in the direction of the movement balances the aerodynamic drag. The bird obtains the power to fly by decreasing its potential energy, which is later recovered by taking advantage of the air flows existing in the Earth atmosphere, or by using its internal (chemical) energy, through flapping during given phases of the flight in order to recover the lost altitude. This kind of flight has been extensively analysed by many scientists (see, for instance, Pennycuick, 1968, 1972a, 1972b, 1975, 1989; Kerlinger, 1989; Norberg, 1990), and it is the easiest to explain and understand.

Flapping flight is much more complex. The thrust needed to balance aerodynamic drag must be obtained from wing flapping, and although the generation of thrust with flapping wings can be explained by using very simple mathematical models when considering rigid wings (von Holst & Küchemann, 1942; Küchemann & Weber, 1953), the real movement of birds' wings, articulated and highly flexible, is extremely complicated, depending even

* IDR/UPM, Laboratorio de Aerodinámica, E.T.S.I. Aeronáuticos. Universidad Politécnica de Madrid. E-28040 Madrid, Spain.

[1] E-mail: jcalvarez@idr.upm.es.

** SEO. Sierra de Guadarrama. Madrid, Spain.

on flight speed (Gray, 1960). The wing moves upwards and downwards, and, at the same time, moves upstream and downstream with respect to the centre of gravity of the bird. In addition, its shape changes, producing a very complex vortex wake rather different from the one produced by an aircraft or by the gliding flight of a bird (Archer *et al*., 1979; Rayner, 1979a, 1979b; Fejtek & Nehera, 1980; Jones, 1980; Philips *et al*., 1981; DeLaurier, 1993; DeLaurier & Harris, 1993; Vest & Katz, 1996).

Concerning gliding flight, the basic equation of the steady flight dynamics of wings states that, in equilibrium, the aerodynamic lift generated by a wing must be equal to the weight of the flying object, that is:

$$Mg = L = \frac{1}{2}\rho U_\infty^2 S C_l, \qquad (1)$$

where M is the mass, g is the acceleration due to gravity, L is the wing lift, ρ the fluid density, U_∞ the flight speed, S the wing area, and C_l the lift coefficient, which in turn is a function, among others, of the angle of attack of the wing, α. Then, taking into account that both air density, ρ, and wing surface, S, do not change during steady flight, if the flying speed, U_∞, decreases, the lift coefficient, C_l, must be increased accordingly in order to keep the lift unaltered. Otherwise, the lift would be smaller that the weight and horizontal flight would not be possible.

Therefore, at low speeds the value of the lift coefficient must be as high as needed to balance the weight, but unfortunately the maximum value of the lift coefficient, $C_{l\max}$, is limited. The lift coefficient is a function mainly of both the wing geometry and the angle of attack. Then, assuming the geometry is not drastically modified (steady flight), the only possibility of increasing the value of the lift coefficient is by increasing the value of the angle of attack. But this can not be done indefinitely because, at high angles of incidence, separation of the boundary layer takes place and wing airfoils stall.

The great importance of the maximum lift characteristics in landing for determining the wing load of aeroplanes has resulted partly in extensive research on stall and maximum lift coefficients of airfoils and wings, and partly in the development of a variety of methods for the increase of this lift. The two-dimensional stall problems (airfoil stall) have been, compared to three-dimensional stall, well investigated and summarised (McGullough & Gault, 1951).

To increase the maximum value of the lift coefficient, aircraft wings are equipped with high lift devices, usually retractable, which are used both at take-off and landing. High lift devices can be located either at the trailing edge (the different types of flaps) or at the leading edge. High lift devices work either by increasing the airfoil chord, by increasing the airfoil camber (the airfoil curvature) or by controlling the boundary layer, making it more resistant to adverse pressure gradients (Abbot & von Doenhoff, 1959; Smith, 1975).

Birds are also equipped with high lift devices. Trailing edge flaps can be identified in birds with some special tail arrangement, such as *Fragata magnificiens*, *Elanoides furcatus*, and *Hirundo rustica* (von Holst & Küchemann, 1942; Storer, 1948; Kuethe & Chow, 1986), although other explanations have been found for these tail arrangements (Norberg, 1994).

The leading-edge high-lift device of birds is the alula, a set of feathers placed at the thumb (alular digit), which in steady gliding flight is oriented parallel to the leading edge. Depending on both the flight speed and the angle of attack of the wing, the alula is joined to the upper wing surface or it detaches from the wing body, acting like the aircraft slats (a small wing located at the wing leading edge of some aircraft quite similar in function and in shape to the alula). Once deployed, the alula generates a velocity field that is in opposition to the one generated by the airfoil itself (decreasing the air speed at the airfoil upper surface close to the leading edge), so that the high adverse pressure gradient existing at the airfoil upper surface when the angle of attack is large is reduced, and the resistance of the airfoil against stalling is enhanced.

This behaviour is clearly shown in Fig. 1, where the dimensionless pressure distributions measured on the upper surface of an airfoil with and without alula have been plotted. In this plot the variation of the pressure coefficient with the distance along the airfoil chord is shown. Pressure coefficient is defined as

$$c_p(\xi) = \frac{p(\xi) - p_\infty}{\frac{1}{2} p U_\infty^2},$$

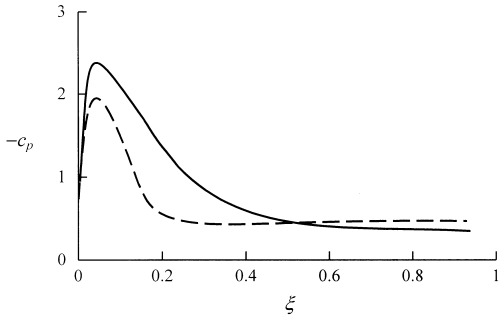

FIG. 1.—Variation along the dimensionless airfoil chord, $\xi = x/c$, of the pressure coefficient $c_p(\xi)$ on the upper surface of a typical bird airfoil *(Columba livia)* at an angle of attack $\alpha = 25^o$. Solid line corresponds to a wing section with alula, whereas the dashed line corresponds to the same wing section but without alula.
[Variación a lo largo de la cuerda adimensional ξ = x/c, *del coeficiente de presión* $c_p(\xi)$ *en el extradós de un perfil típico de ala de ave (*Columba livia) *a un ángulo de ataque* $\alpha = 25^o$. *La línea continua corresponde a un perfil con álula, y la línea a trazos al mismo perfil, pero sin álula.]*

where $p(\xi)$ is the pressure measured at a distance x from the airfoil leading edge, $\xi=x/c$, c being the airfoil chord, p_∞ is static pressure inside the wind tunnel test chamber and $(1/2)\rho U_\infty^2$ is the dynamic pressure (pressure distributions have been measured in the A9 Wind Tunnel of IDR/UPM, on the upper surface of a wing mock-up representing a typical wing section of *Columba livia*; additional details on the pressure distribution measurements can be obtained upon request from the authors).

Alula deflection can be easily observed when birds land on their nests (observation is easier in the case of large birds like storks, because they follow a smooth flight path, moving their wings slowly). Since the aerodynamic performance of the bird depends on its relative velocity with respect to the air, the best conditions for observation probably are during in windy days, with the observer placed upstream of the landing point. The bird which is going to land faces against the wind (so that its relative velocity with respect to ground is small, improving the conditions for observation) and reduces its flight speed by increasing its aerodynamic drag (placing its feet, previously aligned with the velocity vector, perpendicular to the flight path; Pennycuick, 1975). Therefore, the bird must increase its angle of attack to keep the aerodynamic lift unaltered. As the approximation manoeuvre concludes, very close to the nest, the required angle of attack is so high that the wing would stall. But at these high values of angles of attack, in spite of the low velocity, the pressure peak at the leading edge wing is so high that the alula is deflected, preventing wing stalling or at least the stall in the part of the wing protected by the alula. In the case of storks, the observation of the alula deflection is even improved by the fact that alula feathers are black, so that they provide a sharp contrast with respect to the other background feathers that are white.

The alula is a leading-edge, high-lift device whose importance in low-speed flight is well recognised. It has been reported that birds without alula dramatically reduce their ability for take-off and landing (Storer, 1948). The role of the alula in avian flight or at least some aspects of its impact on the wing aerodynamics are to some extent a matter of discussion. The alula is controlled by three muscles (Storer, 1948), which are responsible for its position with respect to the wing. That seems to indicate that the alula could be voluntarily deployed by the bird. On the other hand, since the alula is placed in the vicinity of the suction pressure peak appearing at the leading edge, this suction, increasing with the angle of attack, could cause the automatic detachment of the alula for a given threshold of the angle of attack.

Aiming to clarify the role of the alula in avian steady flight, some representative parameters of the wing geometry and alula position and size of forty species of birds have been measured. In the following, the results of these measurements are reported and the influence of the wing arrangement on the steady gliding flight of birds is analysed. In addition, to clarify if the alula is voluntarily deployed by the bird or by aerodynamic forces, a set of experiments have been performed.

METHODS

As already said, the alula is a leading-edge, high-lift device whose utility is displayed mainly

at high angles of attack, as it happens in landing. Therefore, from the sobe point of view of steady aerodynamics, one could expect this high-lift device to be more important in wings of birds that land and take-off often than in birds that seldom do that. From this point of view, one could expect also that the alula in high aspect ratio wings is less important than in low aspect ratio wings. The reason is that high aspect ratio wings are low induced drag wings which are well adapted for flying in open spaces, whereas low aspect ratio wings seem to be designed for acrobatic flight, which requires high values of the lift coefficient and a wing configuration safe enough against stall (Storer, 1948).

To get additional insight on the relation between the alula and the aerodynamic characteristics of the wings of birds, during the years 1997, 1998 and 1999, different field measurement campaigns have been performed. During these campaigns, several parameters of the wing geometry of almost four hundred and fifty birds, belonging to forty different species living in Spain, have been measured (the biometry method has been published elsewhere, Alvarez *et al*., 1998; Meseguer & Alvarez, 1998). The measured parameters are the following (Fig. 2):

- The mass of the bird, M,
- The length of the extended wing, L_w,
- The maximum wing chord, c_w,
- The length of the alula, L_a,
- The distance between the root of the alula and the wing tip, L_c,
- The bird span, L_b,
- The contours of the extended wings. From these contours, the wing area, S_w, and the total lifting surface of each bird, S_b, have been obtained. The total lifting surface S_b has been defined, according to Pennycuick (1989), as $S_b=2S_w + L_t c_w$, where L_t is the width of the thorax, $L_t=L_b - 2L_w$).

The averaged values of the above-defined parameters, corresponding to the forty different measured species, are listed in the Appendix, in addition to some relevant parameters related to the bird flight capacity (the wing load, $W_l = Mg/S_b$), and to the wing geometry (the wing aspect ratio, $\Lambda = L_b^2/S_b$, and the ratios L_c/L_b and $2L_a/L_w$). In addition, the species listed in the Appendix are labelled as type A, B, C or D, according to the standard wing shapes classification (Saville, 1956; Norberg, 1990). These types are:

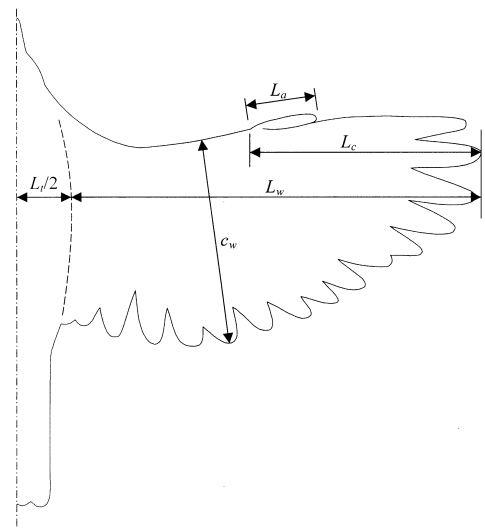

FIG. 2.—Definition of the measured wing parameters. The bird span is $L_b=2L_w+L_t$.
[Definición de los parámetros del ala medidos. La envergadura del ave es $L_b=2L_w+L_t$*.]*

1) Type A, elliptical wing: this kind of wing shape is very efficient at low and moderate speeds. With a low aspect ratio, elliptical wings generate a smooth tip vortex and a uniform pressure a distribution over the wing surface (provided the dimensionless lift distribution along the wing span is elliptical). This wing shape provides good manoeuvrability and is characteristic of small birds with active (flapping) flight. Birds that move in dense forest and vegetation, where small span and accurate flight control are quite necessary, have also this type of wing.
2) Type B, high speed wing: it is characterised by low camber airfoils, moderate high aspect ratio, pronounced sweepback of the leading edge and sometimes even of the trailing edge. The wing tip is not generally slotted. Birds with high flight speeds, moving in open spaces, have this type of wing. Birds with other types of wing try to approach the type B shape, closing the slotted wing tips, when they need to reach high speeds.

3) Type C, high aspect ratio wing: this wing shape is the typical wing of the birds that use to fly over water surfaces. These wings are nicely adapted for dynamic soaring (Pennycuick, 1975), because of their high aerodynamic efficiency. Type C wings could be labelled also high speed soaring wings.
4) Type D, high lift wing: the wings belonging to this type are characterised by a slotted wing tip, moderate aspect ratio and pronounced camber airfoils. Type D wings are very efficient at low speeds and they seems to be especially adapted for soaring flight over land, where air flows are mainly vertical (Pennycuick, 1975). These wings could be also described as low speed soaring wings.

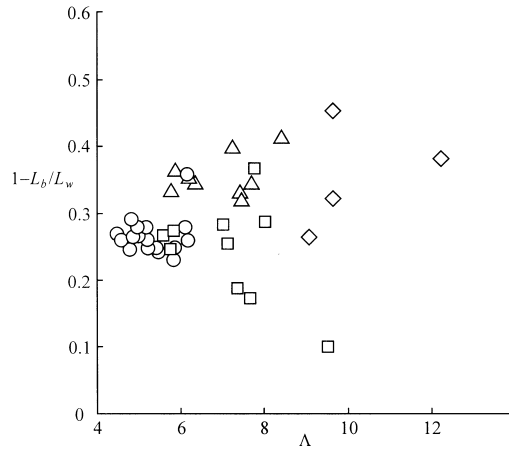

FIG. 3.—Variation with the aspect ratio, Λ, of the ratio of the root alula position to the wing length, $1-L_c/L_w$. Symbols indicate the type of wing according to the following key: circles: type A (elliptical wings), squares: type B (high speed wings), rhombi: type C (high aspect ratio wings), triangles: type D (high lift wings).
[Variación con el alargamiento, Λ, del cociente entre la posición de la raíz del álula y la longitud del ala, $1-L_c/L_w$. Los símbolos identifican el tipo de ala de acuerdo con la clave siguiente: círculos: tipo A (alas de forma en planta elíptica), cuadrados: tipo B (alas para alta velocidad), rombos: tipo C (alas de gran alargamiento), triángulos: tipo D (alas de alta sustentación).]

RESULTS AND DISCUSSION

The data on geometrical parameters listed in the Appendix allows to derive some conclusions on the aerodynamics of bird wings. For instance, in Fig. 3, the variation with the bird aspect ratio Λ of the ratio $1-L_c/L_w$ is presented. This plot shows that practically all Type A wings have the alula placed at distances from the wing root ranging from 0.25 to 0.3 times the wing span. Such distance is smaller in the case of type B wings (observe the extreme value measured in the case of *Apus apus*) and larger in the case of Type D wings, as well as in the case of Type C wings.

For the time being, if only steady flight is considered and flapping is not taken into account, the relationship between alula position and flight behaviour seems to be a consequence of both aerodynamic and structural requirements. According to the data plotted in Fig. 3, extreme values of the alula position along the wing span have been found in the case of type B wings (high speed wings), where the alula is closer to the wing root than in other types of wings, and in type D wings (low speed soaring wings), in which the alula is far from the wing root.

The alula is the border between two regions of the wing, which are clearly differentiated. In the inner part of the wing, between the wing root and the alula, the wing structure is supported by skeletal elements (humerus, radius and ulna) forming a mechanical structure of high resistance. Beyond the alula, the wing is formed by feathers, less resistant than bones from a mechanical point of view. This structural arrangement has a major impact on the aerodynamics of the wing airfoils. Close to the wing root, where the structural elements are the bones, the airfoils are thick, whereas the thickness is very small as one approaches the wing tip.

At high speeds, the lift coefficient needed for flight is small and in consequence the angle of attack of the wing is small. Since in this case stalling is not the driving criterion for wing design, wing airfoils can be thin. On the other hand, if the bird mass is small (the wing load will be also small), structural requirements are not a too severe constraint for the wing structure, so that feathers are resistant enough to conform the wing shape (this seems to be the case for type B wings).

Thick airfoils provide pressure distributions with smooth adverse pressure gradients, so that these airfoils are better adapted than thin airfoils for low speed flight (which means high angles of attack). In addition a high mass bird (high wing load) seems to indicate the need for a reinforced structure extending over a part of the wing greater than in low wing load birds, which could explain why type D wings have the alula more separated from the wing root than other types of wings.

Before getting on with the information presented in the Appendix, it would be convenient to remember some basic additional details concerning wing aerodynamics. Two of the main parameters that define the steady aerodynamic characteristics of a wing are the aspect ratio, Λ, and the wing load, $W_l=Mg/S_b$. From the point of view of aerodynamics, a high aspect ratio wing is nicely adapted to minimum energy consumption flight. In a steady flight, the required power is equal to U_∞ times the aerodynamic drag, which in turn is the dynamic pressure multiplied both by a surface of reference, S_b, and by the drag coefficient, C_D:

$$D = \frac{1}{2}\rho U_\infty^2 S_b C_d \qquad (2)$$

The drag coefficient can be expressed as $C_D=C_{Do}+C_{Di}$, where C_{Do} is the drag coefficient due to viscous friction and the C_{Di} is the induced drag, that is related to the wing lift coefficient C_L through the expression:

$$C_{Di} = \frac{C_L^2}{\pi\Lambda}(1+\kappa) \qquad (3)$$

κ being a parameter that, to a first approximation, depends on the wing shape and on the distribution of angles of attack along the wing span (Abbott & von Doenhoff, 1959). The above expression clearly shows that the higher the aspect ratio the smaller is the induced drag coefficient is and, thus, the power needed for flight. On the other hand, the lift coefficient, related to the wing load through the expression:

$$W_l = \frac{Mg}{S_b} = \frac{1}{2}\rho U_\infty^2 C_L, \qquad (4)$$

so that, for a given flight speed, a high wing load implies the need of generating high values for the lift coefficient.

High aspect ratio wings are especially adapted for gliding flight, and one could expect that any flying object provided with this type of wing follows smooth paths through the air, avoiding abrupt manoeuvres. As the lift is distributed along the wing span, the bending torque at the wing root section will increase as the wing aspect ratio increases. The bending torque will be even higher during manoeuvres, directly depending on the load factor.

This smooth flight behaviour seems to indicate that birds with high aspect ratio wings are poorly adapted for flying between trees or in other environments with obstacles. One could expect that high-aspect-ratio-winged birds expend most of their time flying in open spaces, with infrequent take-offs and landings. Therefore, from the point of view of aerodynamics, the need for high values of the lift coefficient when high-aspect-ratio wings are used is, to some extent, secondary. Since birds are vertebrates that have optimised their body structure to improve their aerodynamic performances, it would be a waste of aerodynamic resources that birds that do not need high lift coefficients would developed large high lift devices like the alula. In consequence, the alula should be less important as the aspect ratio grows.

From the data presented in the Appendix, the ratio $2L_a/L_b$ versus the aspect ratio Λ has been plotted in Fig. 4. This plot shows that the length of the alula is a fraction of the wing span that decreases as the aspect ratio increases in accordance with the above reasoning.

Note that in Fig. 4, the different species of birds are ordered according to their wing type. Birds having wings of type A are characterised by low values of the aspect ratio and high values of the alula length to wing span ratio, $2L_a/L_b$. That means that these birds, usually of small size, are equipped with alulas that are large with respect to the bird span, which can be understood by taking into account the flying behaviour of type A wing birds, with frequent take-offs and landings.

The geometry characteristics of the wing of birds provided with high aspect ratio wings (type C) are rather different. In this case, the ratio $2L_a/L_b$ is almost half that of a typical value for type A wing birds. It seems that for this

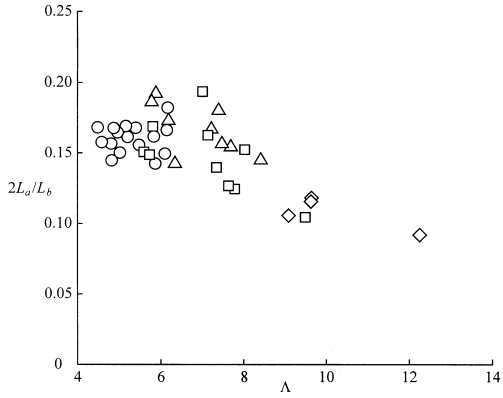

FIG. 4.—Variation with the aspect ratio, Λ, of the ratio of the alula length to the bird span, $2L_a/L_b$. Symbols indicate the type of wing according to the following key: circles: type A (elliptical wings), squares: type B (high speed wings), rhombi: type C (high aspect ratio wings), triangles: type D (high lift wings). *[Variación con el alargamiento,* Λ*, del cociente entre la longitud del álula y la envergadura del ave,* $2L_a/L_b$*. Los símbolos identifican el tipo de ala de acuerdo con la clave siguiente: círculos: tipo A (alas de forma en planta elíptica), cuadrados: tipo B (alas para alta velocidad), rombos: tipo C (alas de gran alargamiento), triángulos: tipo D (alas de alta sustentación).]*

kind of birds, the alula is a secondary element with less impact on the aerodynamic performances of type C wings. The existence of small length alulas in type C wings seems to be in agreement with the aerodynamics requirements for this kind of birds. Most of type C wing birds are pelagic birds expending most of their lives flying over water surfaces, with a low rate of take-off and landing operations, so that they do not need as effective high lift devices as type A wing birds need.

An intermediate position between birds with wings of type A and birds with type C wings is filled by type B wing birds. This last type of wing correspond to birds that use to fly at high speeds, expending a high percentage of their lives flying, with few take-offs and landings.

The high lifts that can reach type D wings require some explanation. They have wings with not too high aspect ratios but they are provided with relatively large alulas. This can be explained by considering that these birds use to fly at low speeds, so that for a given value of the wing load they need higher values of the lift coefficient than birds that fly at higher speeds.

Concerning wing loads, the variation with the alula length of the wing load has been represented in Fig. 5. The points representing the different bird species are almost aligned along two different lines. The alula length is larger as the wing load increases, which is in agreement with the behaviour predicted by equation (4), as well as with the expected role of the alula as a high lift device in the flight mechanics of birds. Equation (4) states that once the flight speed is fixed, the lift coefficients must be higher as the wing load grows. Since increasing the value of the lift coefficient means increasing the value of the angle of attack, the possibility of wing stalling grows accordingly.

Type D wing birds show an anomalous behaviour when compared with other birds. As already pointed out, for the same value of the wing load, they have alula lengths that are higher than the alula lengths of other types of birds. The reason that justifies such a remarkable aerodynamic difference, as already explai-

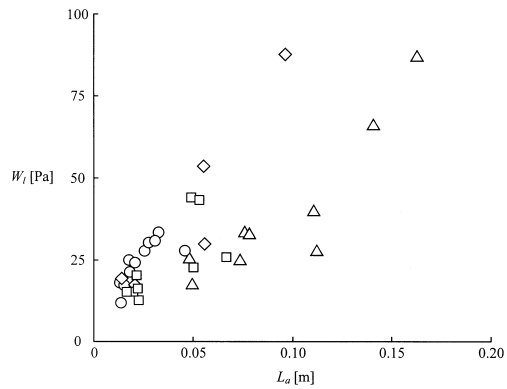

FIG. 5.—Variation with the alula length, L_a, of the wing load, $W_l=Mg/S_b$. Symbols indicate the type of wing according to the following key: circles: type A (elliptical wings), squares: type B (high speed wings), rhombi: type C (high aspect ratio wings), triangles: type D (high lift wings).
[Variación con la longitud del álula L_a *de la carga alar,* $W_l=Mg/S_b$*. Los símbolos identifican el tipo de ala de acuerdo con la clave siguiente: círculos: tipo A (alas de forma en planta elíptica), cuadrados: tipo B (alas para alta velocidad), rombos: tipo C (alas de gran alargamiento), triángulos: tipo D (alas de alta sustentación).]*

ned, could be that these type D wing birds use to glide at low speeds, so according to equation (4), they need to reach high lift coefficients in flying conditions safe enough against stalling.

Additional wind tunnel experimental results

Since the alula seems to play a capital role in the steady flight of birds at low speeds, a question arises. Is the alula deployed voluntarily by the bird or by aerodynamic forces? To answer this question, sets of very simple experiments have been performed, aiming to compare the mechanism of alula deflection in living and in dead birds. The hypothesis to be checked is that, if no differences are observed between living and dead birds, alula deflection is not voluntarily controlled.

To perform the experiments described, a very small wind tunnel (used for educational activities at IDR/UPM) has been used. This has been modified to meet experimental requirements. The diffuser downstream of its test chamber has been removed, so that a laminar jet of air 0.04 m width and 0.30 m height is obtained (turbulence intensity in the potential core of the jet was smaller than 1%). One of the wings of the bird to be tested is placed inside the air stream and the aerodynamic behaviour of the wing is observed.

Birds have been kept at the desired position directly by an operator. The operator holds the bird with one of its wings extended, the root section and the tip section being parallel the air jet impinging on the wing sections where the alula is located (Fig. 6). It must be pointed out that the width of the potential core of the jet (the region with constant velocity), is of the same order as the alula length, and that this potential core extends far downstream of the wing trailing edge (the two lateral mixing layer joint far downstream of the wing). In all experiments where living birds were used, the birds were kept immobile inside a cloth bag with two slots, one for the wing that is tested and a second for the bird's head.

The experimental procedure has been as follows: for each selected value of the air jet velocity, the angle of attack is slowly increased until the deployment of the alula is observed. The same experimental sequence is repeated at different air speeds (the maximum air speed

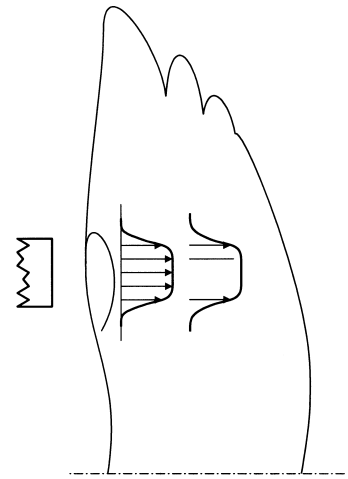

FIG. 6.—Sketch of a pigeon wing and the air jet supplied by the small wind tunnel used in the experiments with pigeons.
[Esquema del ala de una paloma y del chorro de aire generado por el pequeño túnel aerodinámico empleado en los experimentos con palomas.]

that can be obtained in this wind tunnel is near 15 $m \cdot s^{-1}$). The angles of attack have been measured by visual comparison of the wing position with respect an adjustable reference. This method gives a high uncertainty in the angle of attack measurements (±5°, according to some previous tests performed), but this accuracy has been considered enough for the purposes of this experimental study.

Three pigeons *Columba livia* have been tested for the experiment. There are two reasons that advise the employment of pigeons in experimental work: their availability and that this species has been used in the past by other investigators, either for experimentation (Pennycuick, 1968) or for theoretical analysis (Vest & Katz, 1996). Two pigeons were alive (samples number 1 and number 2), whereas the third one was already dead (sample number 3). The dead pigeon, coming from a hunting club, had been killed the day before the tests. It was kept at room temperature during the period between actual death and tests (less than 24 hours). Before testing, its wings were carefully inspected to assure that they had not been previously injured. The geometry of the pigeon wings used in experiments are summarised in Table 1.

TABLE 1

Wing characteristics of the tested pigeons *(Columba livia).*
[Características de las alas de las palomas empleadas en los ensayos (Columba livia).*]*

	Sample No. 1 *[Ejemplar núm. 1]*	Sample No. 2 *[Ejemplar núm. 2]*	Sample No. 3 *[Ejemplar núm. 3]*
Wing span (m) *[Envergadura (m)]*	0.303	0.314	0.294
Maximum wing chord (m) *[Cuerda máxima (m)]*	0.119	0.131	0.114
Alula length (m) *[Longitud del álula (m)]*	0.054	0.055	0.054
Alula chord (m) *[Cuerda del álula (m)]*	0.019	0.020	0.019

Experimental results obtained were practically the same for the three specimens tested. At low velocities, below 12 $m \cdot s^{-1}$ for living birds (samples number 1 and number 2), no alula deflections were observed (the value of the angle of attack is indifferent), but at velocities higher than 12 $m \cdot s^{-1}$, the alula detached from the wing body. In the case of the dead bird (sample number 3), the behaviour was the same, but the limiting velocity was 10 $m \cdot s^{-1}$. In all cases, the tip of the alula separated from the wing a distance of the order of the alula chord (some 15% of the airfoil's chord).

The small difference between the behaviour of living pigeons and the dead pigeon is probably due to experimental conditions, rather different from those presented in a real flight. Probably, to keep root and tip sections in contact with the hands of the operator was a very severe constraint for living birds. The living birds felt a strange body touching their wing at the root section, which probably stressed them, causing the stiffening of their extended wings. Therefore, alula deflection takes place at higher velocities (or higher angles of attack) than the corresponding values without stressing.

In all the tested cases, as the alula deflects, a dramatic change in the fluid configuration around the wing has been observed. At low angles of attack, without boundary layer separation, fluid particles passing close enough the airfoil upper surface follow paths which resemble the airfoil upper surface geometry. The fluid flow can be easily visualised by using wool tufts that become aligned to the local velocity (see Fig. 7a). In our experimental conditions, at high angles of attack, but before alula separation, the airfoils are stalled, boundary layer is separated and a wide turbulent wake is formed. In this situation, wool tufts placed at the upper wing surface show a random orientation, and they adopt an orientation even inverted with respect to the unperturbed free stream (Fig. 7b). Once deflection of the alula occurs, the velocity field induced by the alula strongly modifies the fluid configuration. The point where boundary layer separates is swept downstream, the boundary layer reattaches and the airfoil is no longer stalled. Wool tufts become again parallel to the wing surface and oriented as can be expected in a non stalled airfoil (Fig. 7c).

In any case, the performed experiments allow us to conclude that the aerodynamic forces around the airfoil play an important role in alula deflection. In effect, as the angle of attack grows, the suction peak existing in the vicinity of the leading edge grows accordingly. This suction generates a lift force on the alula that tends to detach it from the wing body. At a certain velocity the deployment starts, although at the very beginning the separation is almost imperceptible. Further increases of either the air velocity or the angle of attack, causes the sudden separation of the alula from the wing body, the final position being, as already said, with the alula tip separated a distance of the order of the maximum alula chord. It must be remarked that this behaviour was the same, no matter if the pigeons were dead or alive (although the minimum velocity at which the deflection of the alula was observed was slightly smaller in

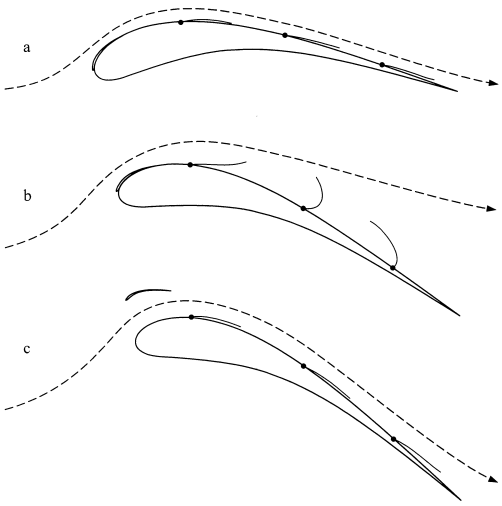

FIG. 7.—Flow pattern over the upper surface of a typical airfoil of a *Columba livia* wing at different angles of attack.
[Configuración fluida en el extradós de un perfil de ala típico de Columba livia *a distintos ángulos de ataque.]*

the case of the dead bird), so that we conclude that alula deflection is caused by aerodynamic forces and not voluntarily deployed by the bird, although additional experimental evidence from new tests with other birds would be convenient.

ACKNOWLEDGEMENTS.—The authors are indebted to J. M. Perales (IDR/UPM), J. Fimia (SEO-HALCYON), M. Rendón (Fundación de la Laguna de Fuente de Piedra, Málaga, Spain) and to the Spanish organisations «Grupo de Recuperación de la Fauna Autóctona» (GREFA, Madrid), «Grup Balear d'Ornitologia i Defensa de la Naturalesa» (GOB, Palma de Mallorca) and «Greenpeace-Spain» (Proyecto ZORBA GP VII, Palma de Mallorca).

BIBLIOGRAPHY

ABBOTT, I. & VON DOENHOFF, A. E. 1959. *Theory of Wing Sections*. Dover Publications, Inc. New York.

ÁLVAREZ, J. C., PÉREZ, A. & MESEGUER, J. 1998. Biometría de la pardela cenicienta (*Calonectris diomedea*) y paiño común (*Hydrobates pelagicus*). *Anuari Ornitologic de les Balears*, 12 : 17-28.

ARCHER, R. D., SAPUPPO, J. & BETTERIDGE, D. S. 1979. Propulsion characteristics of flapping wings. *Aeronautical Journal*, 83: 355-371.

DELAURIER, J. D. 1993. An aerodynamic model for flapping-wing flight. *Aeronautical Journal*, 97: 125-130.

DELAURIER, J. D. & HARRIS, J. M. 1993. A study of mechanical flapping-wing flight. *Aeronautical Journal*, 97: 277-286.

FEJTEK, I. & NEHERA, J. 1980. Experimental study of flapping wing lift and propulsion. *Aeronautical Journal*, 84: 28-33.

GRAY, J. 1960. *Animal Locomotion*. Weidenfeld & Nicolson. London.

JONES, R. T. 1980. Wing flapping with minimum energy. *Aeronautical Journal*, 84: 214-217.

KERLINGER, P. 1989. *Flight Strategies of Migrating Hawks*. The University of Chicago Press. Chicago.

KÜCHEMANN, D. & WEBER, J. 1953. *Aerodynamics of Propulsion*. McGraw Hill Publishing Co. Ltd. New York.

KUETHE, A. M. & CHOW, C. Y. 1986. *Foundations of Aerodynamics*. John Wiley & Sons. New York.

MCGULLOUGH, G. B. & GAULT, D. E. 1951. *Examples of three representative types of airfoil-section stall at low speed*. NACA TN 2502. National Advisory Committee for Aeronautics. Washington.

MESEGUER, J. & ALVAREZ, J. C. 1998. El álula: un dispositivo de borde de ataque para el vuelo a baja velocidad de las aves. *Ingeniería Aeronáutica y Astronáutica*, 352: 2-9.

NORBERG, R. A. 1994. Swallow tail streamer is a mechanical device for self-deflection of tail leading edge, enhancing aerodynamic efficiency and flight manoeuvrability. *Proceedings of the Royal Society of London*, 257: 227-233.

NORBERG, U. M. 1990. *Vertebrate Flight*. Springer Verlag. Berlin.

PENNYCUICK, C. 1968. A wind tunnel study of gliding flight in the pigeon *Columba livia*. *Journal of Experimental Biology*, 49: 509-526.

PENNYCUICK, C. 1972a. *Animal Flight*. Edward Arnold Publishers Ltd. London.

PENNYCUICK, C. 1972b. Soaring behaviour and performance of some East African birds, observed from a motor-glider. *Ibis*, 114: 178-219.

PENNYCUICK, C. 1975. Mechanics of flight. In, D. Farner & J. R. King (Eds.): *Avian Biology*, Vol. V, pp. 1-75. Academic Press. New York.

PENNYCUICK, C. 1989. *Bird Flight Performance. A Practical Calculation Manual*. Oxford University Press. Oxford.

PHILIPS, P. J., EAST, R. A. & PRATT, N. H. 1981. An unsteady lifting line theory of flapping wings with application to the forward flight of birds. *Journal of Fluid Mechanics*, 112: 97-126.

RAYNER, J. M. V. 1979a. A vortex theory of animal flight. Part 1. The vortex wake of a hovering animal. *Journal of Fluid Mechanics*, 91: 697-730.

RAYNER, J. M. V. 1979b. A vortex theory of animal flight. Part 2. The forward flight of birds. *Journal of Fluid Mechanics*, 91: 731-763.

SAVILLE, D. B. O. 1956. Adaptative evolution in avian flight. *Evolution*, 11: 212-214.

SMITH, A. M. O. 1975. High-lift aerodynamics. *Journal of Aircraft*, 12: 501-531.

STORER, J. H. 1948. *The Flight of Birds.* Cranbrook Press. Michigan.

VEST, M. S. & KATZ, J. 1996. Unsteady aerodynamic model of flapping wings. *AIAA Journal*, 34: 1435-1340.

VON HOLST, E. & KÜCHEMANN, D. 1942. Biological and aerodynamical problems of animal flight. *Journal of the Royal Aeronautical Society*, 40: 39-56.

[Recibido: 28-12-00]
[Aceptado: 25-5-01]

APPENDIX

Average value, *av*, and standard deviation, *sd*, of the measured wing parameters; *N*: number of measured samples, c_w: maximum wing chord, L_a: length of the alula, L_c: distance between the alula root and the wing tip, L_b: bird span, between the alula root and the wing tip to the extended wing length ratio, $2L_a/L_b$: alula length to bird span ratio.
[Valor medio, av, *y desviación típica,* sd, *de los parámetros medidos en las alas;* N: *número de ejemplares medido, extendida,* c_w: *cuerda máxima,* L_a: *longitud del álula,* L_c: *distancia entre la raíz del álula y el borde marginal del ala,* Λ: *alargamiento* ($\Lambda = L_b^2/S_b$), L_c/L_w: *relación entre la distancia desde la raíz del álula al borde marginal y la*

			M [kg]		L_w [m]		c_w [m]		L_a [m]		L_c [m]	
	N	*WS*	*av*	*sd*	*av*	*sd*	*av*	*sd*	*av*	*sd*	*av*	*sd*
Calonectris diomedea	14	C	0,64	0,06	0.56	0.02	0.12	0.01	0.05	0.00	0.35	0.00
Hydrobates pelagicus	10	C	0.02	0.00	0.16	0.00	0.04	0.00	0.01	0.00	0.12	0.00
Bubulcus ibis	13	D	0.38	0.05	0.41	0.01	0.15	0.00	0.07	0.00	0.25	0.00
Ciconia ciconia	10	D	3.01	0.47	0.90	0.03	0.30	0.01	0.14	0.00	0.53	0.02
Phoenicopterus ruber	15	C, B	2.63	0.58	0.76	0.04	0.20	0.01	0.09	0.00	0.41	0.02
Milvus migrans	2	D	0.78	0.02	0.65	0.02	0.22	0.00	0.11	0.00	0.44	0.00
Gyps fulvus	8	D	7.35	0.50	1.08	0.06	0.43	0.01	0.16	0.01	0.70	0.02
Hieraaetus pennatus	e	D	0.83	0.26	0.55	0.03	0.20	0.00	0.11	0.00	0.37	0.02
Falco naumanni	13	D	0.12	0.02	0.30	0.01	0.10	0.00	0.05	0.00	0.21	0.02
Falco tinnunculus	4	B	0.17	0.03	0.32	0.01	0.11	0.00	0.06	0.00	0.23	0.01
Burhinus oedicnemus	2	B	0.35	0.10	0.35	0.00	0.11	0.00	0.04	0.00	0.22	0.01
Larus ridibundus	11	C	0.27	0.02	0.44	0.02	0.12	0.00	0.05	0.00	0.30	0.01
Columba livia	5	B	0.26	0.07	0.30	0.01	0.11	0.00	0.05	0.00	0.22	0.01
Tyto alba	3	D	0.29	0.04	0.44	0.01	0.15	0.00	0.07	0.00	0.29	0.00
Otus scops	4	D	0.07	0.01	0.23	0.00	0.09	0.00	0.04	0.00	0.14	0.00
Athene noctua	6	D	0.12	0.02	0.23	0.01	0.10	0.00	0.04	0.00	0.16	0.00
Turdus philomelos	7	A	0.07	0.00	0.15	0.00	0.08	0.01	0.02	0.00	0.11	0.01
Strix aluco	4	D	0.42	0.08	0.41	0.01	0.17	0.00	0.07	0.00	0.26	0.01
Apus apus	3	B	0.03	0.00	0.19	0.00	0.05	0.00	0.02	0.00	0.17	0.00
Alcedo atthis	4	A	0.03	0.00	0.12	0.00	0.05	0.00	0.02	0.00	0.07	0.00
Hirundo rustica	6	B	0.01	0.00	0.14	0.00	0.05	0.00	0.02	0.00	0.12	0.00
Delichon urbica	5	B	0.01	0.00	0.13	0.00	0.04	0.00	0.01	0.00	0.10	0.00
Motacilla cinerea	8	B	0.01	0.00	0.11	0.00	0.05	0.00	0.02	0.00	0.08	0.00
Motacilla alba	19	B	0.02	0.00	0.12	0.00	0.06	0.00	0.02	0.00	0.08	0.01
Troglodytes troglodytes	6	A	0.01	0.00	0.06	0.00	0.04	0.00	0.01	0.00	0.04	0.00
Erithacus rubecula	9	A	0.01	0.00	0.09	0.00	0.05	0.00	0.01	0.00	0.07	0.00
Turdus merula	8	A	0.08	0.00	0.16	0.00	0.08	0.00	0.03	0.00	0.12	0.00
Cettia cetti	5	A	0.01	0.00	0.08	0.00	0.05	0.00	0.01	0.00	0.06	0.00
Sylvia borin	8	A	0.02	0.00	0.10	0.01	0.05	0.00	0.01	0.00	0.07	0.00
Sylvia atricapilla	16	A	0.02	0.00	0.09	0.00	0.05	0.00	0.01	0.00	0.07	0.00
Phylloscopus collybita	27	A	0.00	0.00	0.08	0.00	0.04	0.00	0.01	0.00	0.06	0.00
Phylloscopus trochilus	36	A	0.01	0.00	0.08	0.00	0.04	0.00	0.01	0.00	0.06	0.00
Ficedula hypoleuca	3	A	0.01	0.00	0.10	0.00	0.05	0.00	0.01	0.00	0.08	0.00
Parus major	9	A	0.01	0.00	0.10	0.00	0.06	0.00	0.01	0.00	0.07	0.00
Pica pica	6	A	0.17	0.01	0.25	0.01	0.13	0.01	0.04	0.00	0.18	0.00
Sturnus unicolor	4	A	0.08	0.00	0.17	0.00	0.08	0.00	0.23	0.00	0.13	0.00
Passer domesticus	6	A	0.02	0.00	0.10	0.00	0.05	0.00	0.02	0.00	0.07	0.00
Fringilla coelebs	9	A	0.02	0.00	0.11	0.00	0.06	0.00	0.02	0.00	0.08	0.00
Carduelis carduelis	16	B	0.01	0.00	0.10	0.00	0.05	0.00	0.01	0.00	0.07	0.00
Carduelis cannabina	2	A	0.01	0.00	0.10	0.00	0.05	0.00	0.01	0.00	0.08	0.00

WS: wing shape according to Saville classification (as explained in the text), *M*: bird mass, L_w: extended wing length, S_w: wing surface, S_b: total lifting surface, W_l: wing load ($W_l = Mg/S_b$), Λ: aspect ratio ($\Lambda = L_b^2/S_b$), L_c/L_w: distance

WS: *tipo de ala de acuerdo con la clasificación de Saville (véase el texto),* M: *masa del ave,* L_w: *longitud del ala* L_b: *envergadura del ave,* S_w: *superficie del ala,* S_b: *superficie sustentadora total,* W_l: *carga alar* ($W_l = Mg/S_b$), *longitud del ala extendida,* $2L_a/L_b$: *relación entre la longitud del álula y la envergadura.]*

L_b [m]		S_w [m^2]		S_b [m^2]		W_l [Pa]		Λ		L_c/L_w		$2L_a/L_b$	
av	*sd*	*av*	*sd*	*av*	*sd*	*av*	*sd*	*av*	*sd*	*av*	*sd*	*av*	*sd*
1.20	0.02	0.055	0.004	0.118	0.008	53.3	3.8	12.238	0.421	0.619	0.019	0.092	0.002
0.35	0.00	0.006	0.000	0.014	0.001	19.2	1.7	9.075	0.427	0.735	0.018	0.105	0.005
0.90	0.02	0.051	0.002	0.113	0.006	33.8	5.7	7.239	0.683	0.600	0.015	0.169	0.008
1.93	0.07	0.206	0.019	0.446	0.037	66.4	10.1	8.402	0.880	0.586	0.011	0.146	0.006
1,68	0.10	0.129	0.014	0.288	0.031	87.5	15.9	9.648	0.394	0.546	0.011	0.115	0.006
1.42	0.01	0.123	0.002	0.272	0.014	28.1	0.5	7.465	0.548	0.678	0.019	0.158	0.007
2.29	0.12	0.388	0.034	0.836	0.073	87.1	9.5	6.345	0.418	0.653	0.056	0.144	0.006
1.22	0.07	0.089	0.005	0.201	0.010	40.1	11.1	7.403	0.514	0.669	0.013	0.182	0.006
0.66	0.03	0.024	0.001	0.054	0.004	22.9	4.0	8.030	0.605	0.714	0.069	0.152	0.010
0.68	0.02	0.032	0.003	0.068	0.008	25.9	6.9	7.006	0.814	0.719	0.035	0.194	0.012
0.78	0.00	0.035	0.000	0.079	0.002	44.0	14.5	7.781	0.318	0.631	0.048	0.125	0.015
0.95	0.04	0.043	0.004	0.093	0.009	29.9	3.3	9.643	0.437	0.679	0.009	0.118	0.006
0.65	0.03	0.026	0.003	0.059	0.007	43.3	5.4	7.136	0.335	0.745	0.024	0.163	0.016
0.94	0.03	0.054	0.003	0.116	0.009	25.3	5.1	7.689	0.444	0.654	0.015	0.156	0.004
0,50	0.01	0.020	0.001	0.044	0.002	17.7	3.2	5.886	0.541	0.633	0.012	0.194	0.014
0.51	0.03	0.020	0.001	0.045	0.003	25.8	5.5	5.784	0.677	0.665	0.029	0.188	0.013
0.35	0.00	0.009	0.000	0.022	0.001	30.4	2.4	5.481	0.303	0.757	0.009	0.156	0.006
0.89	0.02	0.059	0.003	0.131	0.005	33.3	7.4	6.198	0.173	0.645	0.014	0.175	0.011
0.41	0.00	0.008	0.000	0.017	0.001	20.3	4.7	9.503	0.590	0.900	0.006	0.104	0.006
0.27	0.00	0.005	0.000	0.012	0.000	27.9	2.9	6.162	0.294	0.642	0.012	0.183	0.005
0.32	0.00	0.006	0.000	0.014	0.000	12.9	0.7	7.347	0.425	0.812	0.012	0.140	0.009
0.28	0.00	0.004	0.000	0.010	0.000	16.7	1.1	7.647	0.244	0.828	0.018	0.126	0.008
0.25	0.01	0.005	0.000	0.012	0.001	15.2	2.0	5.591	0.304	0.734	0.021	0.151	0.016
0.27	0.00	0.005	0.000	0.013	0.000	16.5	0.7	5.816	0.343	0.726	0.020	0.170	0.014
0.15	0.00	0.002	0.000	0.005	0.000	18.1	1.5	4.474	0.159	0.731	0.025	0.168	0.004
0.22	0.00	0.004	0.000	0.009	0.000	17.2	1.2	5.008	0.239	0.733	0.018	0.151	0.008
0.37	0.01	0.011	0.000	0.026	0.001	30.9	1.0	5.190	0.567	0.741	0.019	0.166	0.008
0.18	0.00	0.003	0.000	0.007	0.001	18.5	0.7	4.586	0.277	0.740	0.019	0.158	0.007
0.23	0.01	0.004	0.000	0.009	0.000	25.0	4.1	6.104	1.166	0.721	0.057	0.150	0.011
0.21	0.00	0.003	0.000	0.008	0.000	21.4	2.1	5.408	0.257	0.753	0.024	0.168	0.013
0.17	0.00	0.002	0.000	0.006	0.000	11.9	1.0	4.784	0.243	0.755	0.038	0.157	0.009
0.19	0.00	0.003	0.000	0.007	0.000	17.1	1.4	5.215	0.350	0.753	0.020	0.161	0.012
0.23	0.00	0.004	0.000	0.009	0.000	15.6	2.5	5.838	0.466	0.769	0.010	0.162	0.003
0.23	0.00	0.005	0.000	0.011	0.000	15.5	1.4	4.810	0.170	0.709	0.028	0.145	0.004
0.55	0.01	0.027	0.003	0.061	0.006	28.0	3.6	4.974	0.300	0.721	0.025	0.165	0.015
0.38	0.01	0.010	0.000	0.024	0.001	33.4	2.2	6.156	0.119	0.740	0.015	0.166	0.006
0.24	0.00	0.004	0.000	0.011	0.000	24.2	2.7	5.158	0.215	0.722	0.014	0.169	0.016
0.24	0.01	0.005	0.000	0.012	0.001	17.6	1.7	4.860	0.534	0.735	0.021	0.168	0.009
0.22	0.00	0.004	0.000	0.009	0.000	15.4	1.0	5.742	0.178	0.755	0.016	0.149	0.005
0.23	0.00	0.004	0.000	0.009	0.000	17.6	0.5	5.865	0.076	0.752	0.000	0.142	0.012